



## MODELING VISCOUS DAMPING IN NONLINEAR RESPONSE HISTORY ANALYSIS OF BUILDINGS

A. Chopra<sup>(1)</sup>, F. McKenna<sup>(2)</sup>

<sup>(1)</sup> Horace, Dorothy, and Katherine Johnson Chair in Engineering, University of California, Berkeley, chopra@berkeley.edu

<sup>(2)</sup> Associate Research Engineer, Pacific Earthquake Engineering Research Center, fmckenna@berkeley.edu

### Abstract

The Rayleigh damping model, which is pervasive in nonlinear response history analysis (RHA) of buildings, is shown to develop “spurious” damping forces and lead to inaccurate response results. We prove that a viscous damping matrix constructed by superposition of modal damping matrices—irrespective of the number of modes included or values assigned to modal damping ratios—completely eliminates the “spurious” damping forces. Based on response results, we conclude that the classical Rayleigh damping model is inappropriate. The two preferred damping models are (1) a modified Rayleigh damping model in which the stiffness-proportional term is based on a  $\mathbf{k}$  that omits contributions from all rotational springs used to model plastic hinges; and (2) a damping matrix defined by superposition of modal damping matrices. The first of these two models is easier to understand and implement, whereas the second model has the advantage that it eliminates the spurious damping forces even if rotational springs that model plastic hinges include damping, as in some widely used computer programs.

*Keywords: Buildings, damping models, response history analysis, spurious damping forces*



## 1. Introduction

Nonlinear response history analysis (RHA) of structures is being increasingly employed in performance-based earthquake engineering. The standard equations that are solved in nonlinear RHA are

$$\mathbf{m}\ddot{\mathbf{u}} + \mathbf{c}\dot{\mathbf{u}} + \mathbf{f}_s(\mathbf{u}) = -\mathbf{m}\boldsymbol{\iota}_x\ddot{u}_{gx}(t) - \mathbf{m}\boldsymbol{\iota}_y\ddot{u}_{gy}(t) - \mathbf{m}\boldsymbol{\iota}_z\ddot{u}_{gz}(t) + \mathbf{p}_{gr} \quad (1)$$

where  $\mathbf{u}$  is the vector of degrees of freedom (DOFs);  $\mathbf{m}$  and  $\mathbf{c}$  are the mass and damping matrices, respectively; the vector  $\mathbf{f}_s(\mathbf{u})$  represents the nonlinear relation between resisting forces and deformations, which includes both material and geometric nonlinearities. (For linear systems  $\mathbf{f}_s = \mathbf{k}\mathbf{u}$ , where  $\mathbf{k}$  is the stiffness matrix.) The right side represents the dynamic excitation:  $\ddot{u}_{gx}(t)$ ,  $\ddot{u}_{gy}(t)$ , and  $\ddot{u}_{gz}(t)$  are the  $x$ -,  $y$ -, and vertical components of earthquake ground acceleration,  $\boldsymbol{\iota}_x$ ,  $\boldsymbol{\iota}_y$ , and  $\boldsymbol{\iota}_z$  are the corresponding influence vectors, and  $\mathbf{p}_{gr}$  represents gravity loads.

It is standard in earthquake dynamics of structures to model the various energy dissipating mechanisms except inelastic hysteresis by the damping forces  $\mathbf{f}_d = \mathbf{c}\dot{\mathbf{u}}$  in Eq. (1). Although calibrated against modal damping ratios estimated from structural motions recorded within the pre-yielding range of response, it is customary to use the same model for nonlinear RHA of structures. This extension is based on the tacit assumption that the previously mentioned energy dissipating mechanisms continue unchanged even after the structure has yielded. Unfortunately, experimental evidence is not available to support or refute this assumption.

Rayleigh damping is the most common—almost pervasive—model for viscous damping in nonlinear RHA of buildings. The damping matrix is expressed as  $\mathbf{c} = a_0\mathbf{m} + a_1\mathbf{k}$  where the coefficients  $a_0$  and  $a_1$  are determined from damping ratios specified in two natural modes of vibration of the structure or at two selected frequencies. Rayleigh damping is computationally attractive because the damping matrix preserves the sparsity pattern of the stiffness matrix and does not require formation of additional matrices.

However, nonlinear RHA of buildings modeled with Rayleigh damping may lead to responses that are physically not plausible [1–3]; for example, large damping moments appear at beam–column joints when structural elements are yielding, with the corollary effect that bending moments computed from  $\mathbf{f}_s(\mathbf{u})$  in beams and columns framing into a joint are not in equilibrium. This problem was first identified by Chrisp [1] and later by Bernal [3]. As will be demonstrated later, this unbalanced moment is entirely associated with the damping force from the stiffness proportional part of the Rayleigh damping model; we will refer to these damping forces as “spurious” for reasons that will become apparent later.

Several ideas to alleviate or reduce these “spurious” damping forces have been proposed: use the tangent stiffness instead of the initial stiffness in Rayleigh damping [4–7], or assign zero damping to the yielding component of each structural member [8, 9]. Furthermore, the requirement on the damping matrix to eliminate the “spurious” damping forces was identified, and two methods to achieve such a damping matrix were proposed [3].

The purpose of this paper is to investigate these spurious damping forces, identify reasons why the use of the tangent stiffness matrix should be abandoned, and present two methods to eliminate spurious damping forces.



## 2. System and Ground Motion

All response results are presented for a variant of the Seattle 20-story moment-resisting steel frame building designed for the SAC project, as described in Ref. [10]. Modal damping ratios are assumed to be 2%. This value is assigned to the first and third modes to determine  $a_0$  and  $a_1$  in Rayleigh damping. When the damping matrix is defined as superposition of modal damping matrices, all 20 modes are included, with  $\zeta_n = 2\%$  in all modes. All response results presented are for the ground motion defined by the se30 record from the 1985 Valparaiso, Chile, earthquake. It was one of the 20 records with an exceedance probability of 2% in 50 years selected for the Seattle site as part of the SAC project.

## 3. Spurious Damping Forces from Rayleigh Damping Model

Consider a structural model that has mass associated with DOFs  $\mathbf{u}_t$ , zero inertia associated with DOFs  $\mathbf{u}_0$ , and external dynamic forces applied only along DOFs  $\mathbf{u}_t$ . This situation is typical in analysis of building frames, where the joint rotation DOFs are usually assigned zero inertia and the effective external forces associated with horizontal ground motion exist along lateral floor displacements,  $\mathbf{u}_t$ , but not in rotational DOFs. Specializing Eq. (1) for an undamped, linearly elastic system and writing in partitioned form:

$$\begin{bmatrix} \mathbf{m}_{tt} & \mathbf{0} \\ \mathbf{0} & \mathbf{0} \end{bmatrix} \begin{Bmatrix} \ddot{\mathbf{u}}_t \\ \ddot{\mathbf{u}}_0 \end{Bmatrix} + \begin{bmatrix} \mathbf{k}_{tt} & \mathbf{k}_{t0} \\ \mathbf{k}_{0t} & \mathbf{k}_{00} \end{bmatrix} \begin{Bmatrix} \mathbf{u}_t \\ \mathbf{u}_0 \end{Bmatrix} = \begin{Bmatrix} \mathbf{p}(t) \\ \mathbf{0} \end{Bmatrix} \quad (2)$$

Because no inertia terms or external forces are associated with DOFs  $\mathbf{u}_0$ , the second equation permits a static relation between  $\mathbf{u}_0$  and  $\mathbf{u}_t$ :

$$\mathbf{u}_0 = -\mathbf{k}_{00}^{-1} \mathbf{k}_{0t} \mathbf{u}_t \quad (3)$$

We demonstrate next that the damping forces in  $\mathbf{u}_0$  DOFs will be zero for a linear systems with Rayleigh damping:

$$\mathbf{c} = a_0 \mathbf{m} + a_1 \mathbf{k} \quad (4)$$

The damping forces are

$$\begin{Bmatrix} \mathbf{f}_{Dt} \\ \mathbf{f}_{D0} \end{Bmatrix} = \begin{bmatrix} \mathbf{c}_{tt} & \mathbf{c}_{t0} \\ \mathbf{c}_{0t} & \mathbf{c}_{00} \end{bmatrix} \begin{Bmatrix} \dot{\mathbf{u}}_t \\ \dot{\mathbf{u}}_0 \end{Bmatrix} \quad (5)$$

Substituting Eq. (4), the damping forces in  $\mathbf{u}_0$  DOFs are given by

$$\mathbf{f}_{D0} = a_1 \left[ \mathbf{k}_{0t} \dot{\mathbf{u}}_t + \mathbf{k}_{00} \dot{\mathbf{u}}_0 \right] \quad (6)$$

Differentiating Eq. (3) with respect to time gives a corresponding equation in velocities that is substituted in Eq. (6) to obtain



$$\mathbf{f}_{D0} = a_1 \left[ \mathbf{k}_{0t} \dot{\mathbf{u}}_t - \mathbf{k}_{00} \mathbf{k}_{00}^{-1} \mathbf{k}_{0t} \dot{\mathbf{u}}_t \right] = \mathbf{0} \quad (7)$$

Although the damping forces in  $\mathbf{u}_0$  DOFs do not exist during linear response of a structure, they develop after the structure deforms into the inelastic range. Because the stiffness-proportional part of Rayleigh damping is based on the initial stiffness matrix, the damping forces are given by Eq. (6), even after yielding of the structure. However, the internal elastic resisting forces are no longer given by  $\mathbf{f}_s = \mathbf{k} \mathbf{u}$ , but by the nonlinear hysteretic function  $\mathbf{f}_s(\mathbf{u})$ . This implies that the tangent stiffness matrix varies with time, Eq. (3) is no longer valid, and the damping forces  $\mathbf{f}_{D0}$  defined by Eq. (6) will no longer be zero. This seems anomalous in the sense that viscous damping moments develop because of yielding of the structural elements, a mechanism that has no causal relationship to viscous damping. It is for this reason that we refer to them as spurious damping forces.

These spurious damping forces are demonstrated in Fig. 1 where the damping moment—normalized by the plastic moment  $M_p$  of the beam—at a joint on the 18<sup>th</sup> floor of the SAC-Seattle 20-story steel moment-resistant frame building is presented as a function of time. This damping moment is equal to the unbalanced moment  $M_u$  at the joint if member forces are computed from  $\mathbf{f}_s(\mathbf{u})$ . Also shown in Fig. 1 are intervals of yielding of the plastic hinge. Observe that moment imbalance exists at a joint if the structure is yielding but decreases quickly when the structure returns to linearly elastic state. The unbalanced moment is implausibly large, almost three times the plastic moment of the beam; thus the computed response of the structure is expected to be in error, as will be confirmed later.

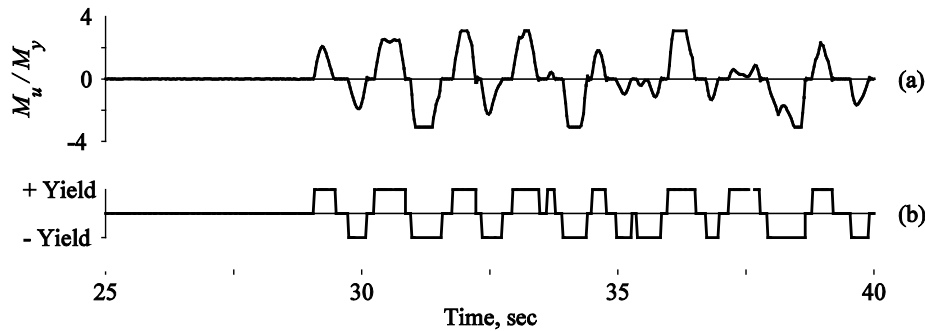


Fig. 1 – Unbalanced moment due to Rayleigh damping at a beam–column joint on the 18<sup>th</sup> floor of the SAC-Seattle 20-story frame due to SE30 ground motion record from the 1985 Valparaiso, Chile, earthquake. Lower part of the figure shows time intervals of yielding (from Ref. [10]).

#### 4 Rayleigh Damping based on Tangent Stiffness

To reduce the unbalanced moments at joints arising from Rayleigh damping, several researchers have proposed to modify the stiffness proportional term by replacing the initial stiffness matrix by the tangent stiffness matrix [4–7], i.e.,

$$\mathbf{c} = a_0 \mathbf{m} + \mathbf{a}_1 \mathbf{k}_t \quad (8)$$

It has been demonstrated that the spurious damping forces are reduced by using the tangent stiffness instead of the initial stiffness. However, defining damping proportional to the tangent stiffness matrix lacks a physical basis and has conceptual implications that are troubling.

To illustrate these issues, we compare the response of an elastoplastic SDF system for two damping models: constant damping coefficient,  $c = \zeta(2m\omega_n) = \zeta(2k/\omega_n)$ —the model used since the inception of research in earthquake response of inelastic systems [11]; and damping coefficient proportional to the tangent stiffness, i.e.,  $c = \zeta(2k_T/\omega_n)$ . We will refer to these models as initial-stiffness-proportional damping and tangent-stiffness-proportional damping, respectively. The second damping model is identical to the first for the elastic branches of the force-deformation curve, but its damping coefficient is zero for the plastic branches. The SDF system considered has the following properties: small amplitude vibration period  $T_n = 0.5$  sec, damping ratio  $\zeta = 5\%$ , and normalized yield strength  $\bar{f}_y = 0.125$ . The deformation response of this system for the two damping models is presented in Fig. 2. Observe that tangent-stiffness-proportional damping leads to larger response because it dissipates no energy while the system is yielding. For this damping model, although the deformation response appears to be reasonable, the variation of damping force with time seems physically unacceptable: the damping force drops suddenly to zero each time yielding occurs, as observed in Fig. 2b. To further understand the implications of this damping model, we focus on a single cycle of response in Fig. 2c-e. Evident are: (1) the sudden drop in damping force; and (2) nonlinear damping force-velocity relation with triangular loops, behavior that lacks a plausible physical basis. As shown Fig. 2e, this damping model does not display complete elliptical loops in the  $f_D - u$  plot that are characteristic of the linear model. Another unacceptable feature of this damping model is that it implies a negative damping coefficient when the member stiffness at large deformations becomes negative.

Because of these conceptual problems, use of the tangent-stiffness-proportional damping model is not recommended, although it greatly reduces the spurious damping forces, as researchers have demonstrated [4–7, 10]. Two preferred approaches to eliminate the spurious damping forces developed in the traditional Rayleigh damping model are presented in the next two sections.

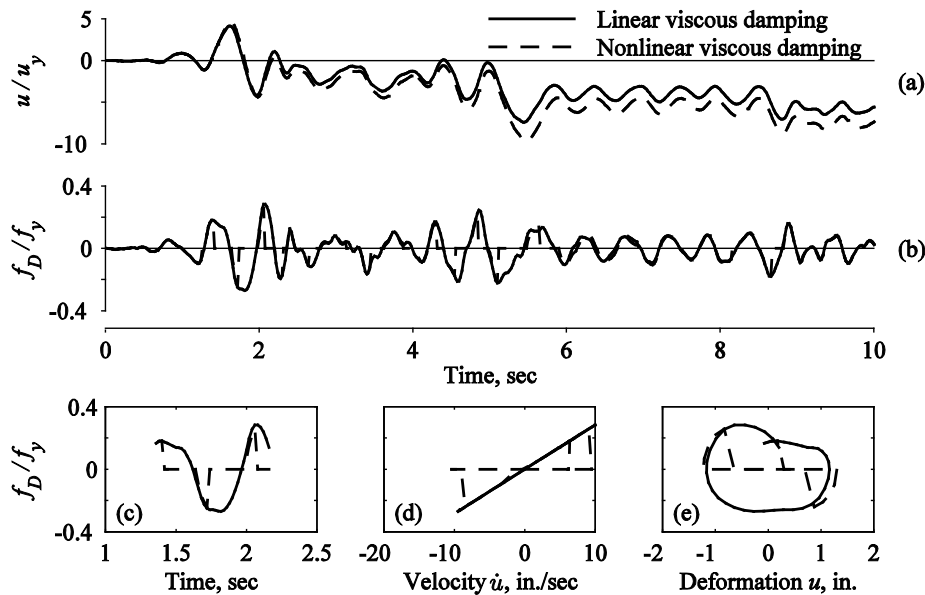


Fig 2 – Response of an elastoplastic SDF system due to El Centro ground motion;  $T_n = 0.5$  sec,  $\zeta = 5\%$ , and  $\bar{f}_y = 0.125$ , (a) deformation; (b, c) damping force, (d) damping force-velocity relation; and (e) damping force-deformation relation. Results are presented for two damping models: linear viscous damping and nonlinear viscous damping with its coefficient proportional to the tangent stiffness (from Ref. [13]).



## 5. Penalty Elements to Model Plastic Hinges

Plastic hinges are typically modeled by rotational springs with, say, bilinear moment-rotation relation. For moment  $M$  less than the yield moment for the beam, the spring should be rigid (i.e., infinitely stiff) to prevent hinge rotation. This idea is implemented by assigning a very high value of initial stiffness to minimize rotation of the rotational spring and its contribution to the flexibility of the beam. If such a high stiffness is included in the  $a_1 \mathbf{k}$  term in Rayleigh damping, a large damping moment will exist even after the hinge yields, resulting in spurious damping forces, as was observed in Fig. 1.

Researchers have demonstrated that penalty-type elements, commonly used to impose constraints at contact or sliding surfaces, are also useful in modeling plastic hinges [8]. Because penalty elements provide only constraints, they should not contain damping. Therefore, stiffness contributions from these penalty elements are not included in the  $a_1 \mathbf{k}$  term of the damping matrix. This approach eliminates the spurious damping forces.

## 6. Modal Damping Model based on Superposition of Modal Damping Matrices

Consider the damping model as a superposition of modal damping matrices [11]:

$$\mathbf{c} = \mathbf{m} \left( \sum_{n=1}^N \frac{2\zeta_n \omega_n}{M_n} \boldsymbol{\phi}_n \boldsymbol{\phi}_n^T \right) \mathbf{m} \quad (9)$$

This model eliminates the spurious damping forces arising in the Rayleigh damping model. Writing Eq. (9) in partitioned form:

$$\mathbf{c} = \begin{bmatrix} \mathbf{c}_{tt} & \mathbf{c}_{t0} \\ \mathbf{c}_{0t} & \mathbf{c}_{00} \end{bmatrix} = \begin{bmatrix} \mathbf{m}_{tt} & \mathbf{0} \\ \mathbf{0} & \mathbf{0} \end{bmatrix} \left[ \sum_{n=1}^N \frac{2\zeta_n \omega_n}{M_n} \begin{Bmatrix} \boldsymbol{\phi}_{nt} \\ \boldsymbol{\phi}_{n0} \end{Bmatrix} \left\langle \boldsymbol{\phi}_{nt}^T \ \boldsymbol{\phi}_{n0}^T \right\rangle \right] \begin{bmatrix} \mathbf{m}_{tt} & \mathbf{0} \\ \mathbf{0} & \mathbf{0} \end{bmatrix} \quad (10)$$

where  $\boldsymbol{\phi}_{nt}$  and  $\boldsymbol{\phi}_{n0}$  are the subvectors of the  $n$ th mode corresponding to the  $\mathbf{u}_t$  and  $\mathbf{u}_0$  DOFs. Multiplying out the matrices on the right side gives

$$\mathbf{c}_{tt} = \mathbf{m}_{tt} \left( \sum_{n=1}^N \frac{2\zeta_n \omega_n}{M_n} \boldsymbol{\phi}_{nt} \boldsymbol{\phi}_{nt}^T \right) \mathbf{m}_{tt} \quad (11)$$

$$\mathbf{c}_{00} = \mathbf{c}_{0t} = \mathbf{c}_{t0} = \mathbf{0} \quad (12)$$

It is clear that the damping matrix of Eq. (9) is of the special form:

$$\mathbf{c} = \begin{bmatrix} \mathbf{c}_{tt} & \mathbf{0} \\ \mathbf{0} & \mathbf{0} \end{bmatrix} \quad (13)$$

With such a damping matrix, the damping forces in the DOFs  $\mathbf{u}_0$  with no mass will always be zero—during both elastic and inelastic regimes of response. This conclusion is valid independent of the number of modes included in Eq. (9) and irrespective of values specified—no matter how small or large—for the modal damping ratios.



However, the implications of not including a particular term in the series of Eq. (9) should be recognized. The  $n$ th term in the summation is the contribution of the  $n$ th mode with its damping ratio  $\zeta_n$ , to the damping matrix. If this term is not included in the series, the resulting damping matrix implies zero damping in the  $n$ th mode. Solution strategies used for numerical integration of equations of motion should be robust enough to work in the presence of zero damping in modes  $J+1$  to  $N$ . Unconditionally stable time stepping procedures, such as the constant average acceleration method should be employed for such applications.

## 7. Related Work

### 7.2 Early Work in RUAUMOKO

The idea of using superposition of modal damping matrices to construct the damping matrix for nonlinear RHA goes back to Chrisp's master's thesis [1] under the supervision of Athol Carr [2]. However, their motivation for introducing this damping model was different than presented in this paper. Our goal was to conform to the special structure of the damping matrix given by Eq. (3), which is achieved by the damping model of Eq. (9), independent of the number of modes and modal damping values. In contrast, their goal was to limit the damping ratio in the very high modes. For this purpose, Carr added two implementations of the damping matrix in his signature software RUAUMOKO [12]; modal damping ratios are (1) constant at all frequencies; and (2) a trilinear function of frequency that is constant at  $\omega$  lower than  $\omega_1$ , varies linearly between  $\omega_1$  and  $\omega_j$ , and then stays constant at  $\omega$  higher than  $\omega_j$ . It was demonstrated that these damping models greatly reduce the spurious damping moments at joints [2].

Unfortunately, the work of Chrisp and Carr did not find widespread adoption, perhaps because it never appeared as a published paper in a prominent journal. As a result, researchers continued to look for a way of reducing the spurious damping forces associated with the Rayleigh damping model.

### 7.2 Earlier Proposals for Damping Matrix of Special Form

Two ways of constructing a damping matrix that conforms to Eq. (13) were proposed in 1994 [3]. The first solution was to use the Caughey series with  $l \leq 0$  terms in Eq. (11.4.11) of Ref. [11]. The second proposal was to first construct the damping matrix with reference to DOFs  $\mathbf{u}_l$  with mass, and then expand this  $\mathbf{c}$  to the full set of DOFs with columns and rows of zeros corresponding to DOFs that have no mass. The condensed damping matrix could be modeled by Rayleigh damping with initial-stiffness-proportional damping and coefficients  $a_0$  and  $a_1$  determined in the usual manner. Neither of these two approaches seem to have been adopted widely, perhaps because they result in a damping matrix that is fully populated, and because the condensed stiffness matrix required in the second approach is *not* computed as part of the standard computation in most general purpose computer programs.

## 8. Influence of Damping Model on Response

Concentrated plasticity is the most common approach to modeling structural elements typical of multistory buildings. This model is based on the assumption that inelastic deformation will be concentrated as plastic hinges at the two ends of a structural element, and the remainder of the element remains linearly elastic.

The earthquake response of a concentrated plasticity model of a building responding into the inelastic range can be greatly influenced by how damping is modeled. Response results will be presented for three damping models: (1) RI, Rayleigh damping based on initial stiffness, Eq. (4); (2) Mod-RI, Modified Rayleigh model without damping in plastic hinges (Section 5); and (3) MODAL, superposition of modal damping matrices, Eq. (9), with damping specified in all 20 modes of dominantly lateral vibration of the 20-story building.



The selected ground motion drives the building significantly into the inelastic range, and its response is greatly influenced by the choice of damping model. This is evident from Fig. 3, where the roof displacement response of the building with its damping defined by three models is presented. The roof displacement of the building with the RI damping model oscillates about the zero-displacement axis, presumably because of the much larger damping resisting force arising from the large initial stiffness of the hinge. In contrast, significant permanent drift is observed in the case of Mod-RI and MODAL damping models, both of which lead to similar response results. As expected based on the preceding observations, the floor displacements, story drifts, and plastic rotations are greatly underestimated if the RI damping model is used. This is shown in Fig. 4 where the height-wise variation of the peak values of these response quantities are plotted; observe that the response results for the other two damping models are similar.

Based on these results, we conclude that the classical Rayleigh damping model is inappropriate for nonlinear RHA of buildings. The preferred damping models are: (1) a modified Rayleigh damping model in which the stiffness-proportional term is based on a  $\mathbf{k}$  that omits contributions from all rotational springs used to model plastic hinges; and (2) a damping matrix defined by superposition of modal damping matrices. The first of these two models is easier to understand and implement, whereas the second model has the advantage that it eliminates the spurious damping forces even if rotational springs that model plastic hinges include damping, as in some widely used computer programs.

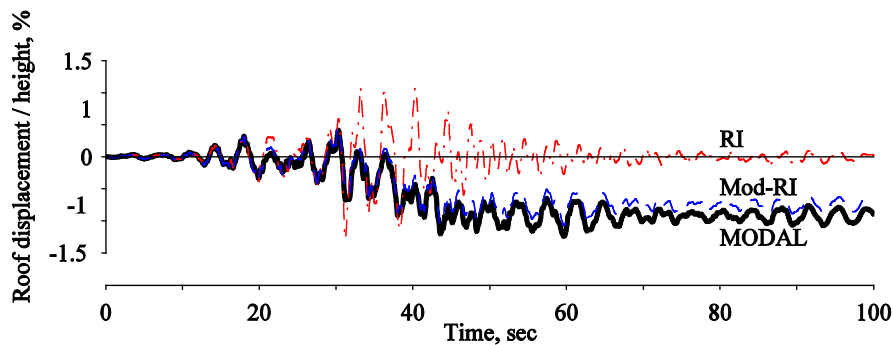


Fig. 3 – Response history of roof displacement due to intense ground motion for three damping models: RI, Mod-RI, and MODAL (with damping specified in all 20 modes); from Ref. [13].

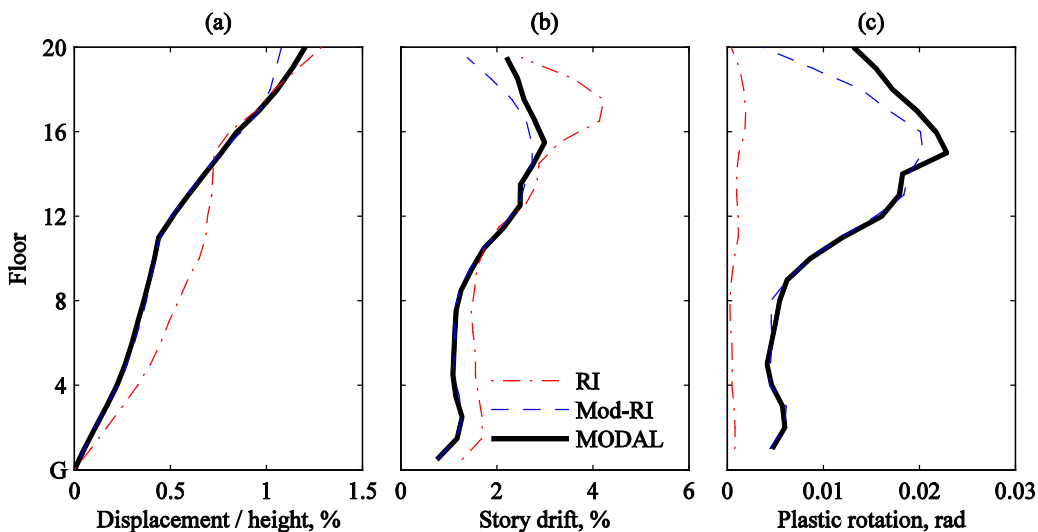


Fig. 4 – Peak values of (a) floor displacements, (b) story drifts, and (c) plastic hinge rotations—at each floor it is the largest value among all hinges—due to intense ground motion for three damping models: RI, Mod-RI, and MODAL (with damping specified in all 20 modes); from Ref. [13].



## 9. Limitations of Linear Viscous Damping

Damping forces can be unrealistically large if the linear viscous damping model is used in nonlinear RHA. This problem, which has been identified in the context of modified Rayleigh damping, arises because yielding of structural elements limits their resisting forces, but no such mechanism exists for limiting the damping forces [8]. In the SDF system mentioned in Section 4, the peak damping force was determined to be almost 30% of the yield strength of the system (Fig. 2b). In contrast, for the corresponding linear system, the ratio of peak values of damping and elastic forces is 10%<sup>+</sup> Hall has proposed the idea of imposing a limit on the damping forces that can develop, resulting in a nonlinear  $\mathbf{f}_D(\dot{\mathbf{u}})$  relation [8]. This idea requires further investigation and development.

## 10. Conclusions

This investigation of modeling viscous damping in nonlinear RHA of buildings with concentrated plasticity at beam-column joints has led to the following conclusions:

1. The Rayleigh damping model causes spurious damping forces, resulting in unbalanced elastic moments at beam-column joints; the source of this problem has been identified.
2. Defining damping matrix proportional to the tangent stiffness matrix lacks a physical basis and is fraught with conceptual problems.
3. The classical Rayleigh damping model is inappropriate for nonlinear RHA of buildings. The preferred damping models are: (1) a modified Rayleigh damping model in which the stiffness proportional term is based on a  $\mathbf{k}$  that omits contributions from all rotational springs used to model plastics hinges; and (2) a damping matrix defined by superposition of modal damping matrices.

## 11. Acknowledgements

The authors are grateful to Professor Filip Filippou for implementing the MODAL damping model in his FEDEASlab code in Matlab, where the full damping matrix is computed. The implementation in OpenSees was validated against this Matlab code. This paper has benefitted from comments by Professors Dionisio Bernal, Athol Carr, and John Hall.

## 11. Copyrights

16WCEE-IAEE 2016 reserves the copyright for the published proceedings. Authors will have the right to use content of the published paper in part or in full for their own work. Authors who use previously published data and illustrations must acknowledge the source in the figure captions.

## 12. References

- [1] Chrisp D (1980). *Damping Models for Inelastic Structures*. Master's Thesis, University of Canterbury, Christchurch, New Zealand.
- [2] Carr AJ (1997). Damping models for inelastic analysis. *Proceedings Asia-Pacific Vibration Conference*, Kyonju, Korea.

---

<sup>+</sup> It can be proven that this ratio is  $2\zeta$  for an SDF system undergoing harmonic vibration at its natural period,  $T_n$ . This result is approximately valid for earthquake response because, when subjected to broad-frequency -band excitations, the system undergoes cyclic motion with dominant period  $T_n$  and slowly varying amplitude.



- [3] Bernal D (1994). Viscous damping in inelastic structural response. *ASCE Journal of Structural Engineering*, **120**(4):1240–1254.
- [4] Leger P, Dussault S (1992). Seismic-energy dissipation in MDOF structures. *ASCE Journal of Structural Engineering*, **118**(6):1251–1267.
- [5] Charney FA (2008). Unintended consequences of modeling damping in structures. *ASCE Journal of Structural Engineering*, **134**(4):581–592.
- [6] Jehel P, Leger P, Ibrahimbegovic A (2014). Initial versus tangent-stiffness based Rayleigh damping in inelastic time history analysis. *Earthquake Engineering and Structural Dynamics*, **43**:476–484.
- [7] Petrini L, Maggi C, Priestley N, Calvi M (2008). Experimental verification of viscous damping modeling for inelastic time history analyses. *Journal of Earthquake Engineering*, **12**(1):125–145.
- [8] Hall JF (2006). Problems encountered from the use (or misuse) of Rayleigh damping. *Earthquake Engineering and Structural Dynamics*. **35**:525–545.
- [9] Zareian F, Medina RA (2010). A practical method for proper modeling of structural damping in inelastic plane structural systems. *Computers and Structures*, **88**:45–53.
- [10] Chopra AC, McKenna F (2016). Modeling viscous damping in nonlinear response history analysis of buildings for earthquake excitation. *Earthquake Engineering and Structural Dynamics*, **45**(2):193–211.
- [11] Chopra AK (2012). *Dynamics of Structures: Theory and Applications to Earthquake Engineering*. 4<sup>th</sup> ed., Prentice Hall, Englewood Cliffs, New Jersey.
- [12] Carr AJ (1982). *Ruamoko Manual, Vol 1: Theory and User's Guide to Associated Programs*. University of Canterbury, Christchurch, New Zealand.
- [13] Chopra AK (2017). *Dynamics of Structures: Theory and Applications to Earthquake Engineering*. 5<sup>th</sup> ed., Prentice Hall, Englewood Cliffs, New Jersey, to be published.